



Universiteit  
Leiden  
The Netherlands

## **The role of fluorescent and hybrid tracers in radioguided surgery in urogenital malignancies**

Vries, H.M. de; Schottelius, M.; Brouwer, O.R.; Buckle, T.

### **Citation**

Vries, H. M. de, Schottelius, M., Brouwer, O. R., & Buckle, T. (2021). The role of fluorescent and hybrid tracers in radioguided surgery in urogenital malignancies. *The Quarterly Journal Of Nuclear Medicine And Molecular Imaging*, 65(3), 261-270.

doi:10.23736/S1824-4785.21.03355-0

Version: Publisher's Version

License: [Licensed under Article 25fa Copyright Act/Law \(Amendment Taverne\)](#)

Downloaded from: <https://hdl.handle.net/1887/3774696>

**Note:** To cite this publication please use the final published version (if applicable).

## REVIEW

IMAGE-GUIDED SURGERY: FROM CLASSICAL TECHNIQUES  
TO NOVEL ASPECTS AND APPROACHESThe role of fluorescent and hybrid tracers  
in radioguided surgery in urogenital malignanciesHielke Martijn DE VRIES<sup>1,2</sup>, Margret SCHOTTELIUS<sup>3</sup>, Oscar R. BROUWER<sup>1,2</sup>, Tessa BUCKLE<sup>1,2,\*</sup><sup>1</sup>Interventional Molecular Imaging Laboratory, Department of Radiology, Leiden University Medical Center, Leiden, the Netherlands; <sup>2</sup>Department of Urology, the Netherlands Cancer Institute, Antoni van Leeuwenhoek Hospital, Amsterdam, the Netherlands; <sup>3</sup>Unit of Translational Radiopharmaceutical Sciences, Department of Nuclear Medicine and Oncology, Centre Hospitalier Universitaire Vaudois (CHUV), Lausanne, Switzerland\*Corresponding author: Tessa Buckle, Interventional Molecular Imaging Laboratory, Department of Radiology, Leiden University Medical Center, Albinusdreef 2, 2300 Leiden, the Netherlands. E-mail: [t.buckle@lumc.nl](mailto:t.buckle@lumc.nl)

## ABSTRACT

The increasing availability of new imaging technologies and tracers has enhanced the application of nuclear molecular imaging in urogenital interventions. In this context, preoperative nuclear imaging and radioactivity-based intraoperative surgical guidance have become important tools for the identification and anatomical allocation of tumor lesions and/or suspected lymph nodes. Fluorescence guidance can provide visual identification of the preoperatively defined lesions during surgery. However, the added value of fluorescence guidance is still mostly unknown. This review provides an overview of the role of fluorescence imaging in radioguided surgery in urogenital malignancies. The sentinel node (SN) biopsy procedure using hybrid tracers (radioactive and fluorescent component) serves as a prominent example for in-depth evaluation of the complementary value of radio- and fluorescence guidance. The first large patient cohort and long-term follow-up studies show: 1) improvement in the SN identification rate compared to blue dye; 2) improved detection of cancer-positive SNs; and 3) hints towards a positive effect on (biochemical) recurrence rates compared to extended lymph node dissection. The hybrid tracer approach also highlights the necessity of a preoperative roadmap in preventing incomplete resection. Recent developments focus on receptor-targeted approaches that allow intraoperative identification of tumor tissue. Here radioguidance is still leading, but fluorescent and hybrid tracers are also finding their way into the clinic. Emerging multiwavelength approaches that allow concomitant visualization of different anatomical features within the surgical field may provide the next step towards even more refined procedures.

(Cite this article as: De Vries HM, Schottelius M, Brouwer OR, Buckle T. The role of fluorescent and hybrid tracers in radioguided surgery in urogenital malignancies. Q J Nucl Med Mol Imaging 2021;65:261-70. DOI: 10.23736/S1824-4785.21.03355-0)

KEY WORDS: Surgery, computer-assisted; Nuclear medicine; Surgical procedures, operative.

With the evolution of imaging technologies and tracers, the applications for nuclear molecular imaging in urogenital interventions are growing rapidly. Historically, surgical planning in urological and gynecological surgery was exclusively based on preoperatively acquired (nuclear medicine-based) imaging results.<sup>1-3</sup> However, in order to provide enhanced clinical value, additional anatomical detail is required to help place these findings into context. A prime example is the fusion of nuclear imaging modalities and radiological modalities, such as the

fusion of single photon emission computed tomography (SPECT) or positron emission tomography (PET) with anatomical information provided by computed tomography (CT) or magnetic resonance imaging (MRI). Such hybrid approaches are a well-accepted means to overcome the limitations of the individual technologies and to generate a “best of both worlds” model.<sup>4,5</sup>

Intraoperative radioguidance can be accomplished based on the same radioactive signals, allowing intraoperative localization of the preoperatively identified lesions.

However, this approach is based on an acoustic readout and does not allow visual confirmation. In contrast, fluorescence guidance has shown great potential in the intraoperative setting by providing optical feedback, in some cases even in real-time. Both radio- and fluorescence guidance have distinct drawbacks, which include inaccuracy in areas that contain a background signal (radioactivity) or a limited degree of signal penetration (fluorescence) and thus their combination into a hybrid approach can be seen as complementary.<sup>6,7</sup>

In this review we discuss the basic principles of fluorescence imaging and the role of fluorescence imaging in radioguided urological and gynecological surgery (Figure 1). To highlight the role of fluorescence in radioguided surgery in urogenital malignancies, fluorescent and hybrid tracers and their clinical applications will be discussed. Here, a special focus was placed on sentinel node (SN) imaging and the up-and-coming possibilities for tumor-specific receptor-targeting approaches. In addition, possibilities for multi-wavelength (or multi-color) applications are discussed.

### Basic principles: fluorescence

In contrast to radiotracers, fluorescent labels require excitation before their emitted signal can be imaged. Every fluorescent dye has a corresponding maximal excitation ( $\lambda_{ex\_max}$ ) and maximal emission wavelength ( $\lambda_{em\_max}$ ); a signature feature that is dependent on the molecular composition of the dye. The  $\lambda_{ex\_max}$  and  $\lambda_{em\_max}$  values are related to the length of the conjugated system, meaning that the maximum value for both may extend up to wavelengths

in the near infrared region. For a fluorescent dye (fluorophore), the intensity of the fluorescent emission is markedly influenced by the intensity of the excitation light source, the degree of absorbance of the excitation light (dictated by the molar extinction coefficient [ $\epsilon$ ]) and the conversion of the absorbed energy into a fluorescent emission (dictated by the quantum yield [ $\phi$ ]). The sum of these factors, combined with the fluorophore concentration, determines the fluorescence brightness.<sup>8</sup>

Unfortunately, conjugated organic molecules such as cyanine dyes tend to interact with each other, which quenches the fluorescence emission.<sup>9,10</sup> As a result, for organic fluorophores, the signal intensity sometimes may even decrease with increasing concentration; an effect that is influenced by the chemical environment of the dye.<sup>9,10</sup> Combined, these photophysical properties can significantly affect a fluorophore's practical usability.<sup>11</sup> It should be noted that seemingly unfavorable photophysical properties do not necessarily rule out the use of a fluorophore (e.g. fluorescein and indocyanine green [ICG]). In some cases, a relatively low fluorescence intensity can be compensated for by using high-intensity light sources, and some wavelengths may even allow accurate diagnostics at low brightness.

The most representative and widely used fluorophores in clinical applications in urogenital malignancies are fluorescein and ICG. These non-conjugated dyes are routinely used in angiography applications<sup>11</sup> and have found their way into urological and gynecological interventions through application during lymphangiography, SN imaging and ureter visualization (Table I).<sup>11-21</sup> Conjugatable dye variants are being applied in clinical trials as part of

Figure 1.—Combined radio and fluorescence guidance. Schematic overview of radioactivity-based preoperative imaging and intraoperative gamma detection and intraoperative fluorescence imaging.

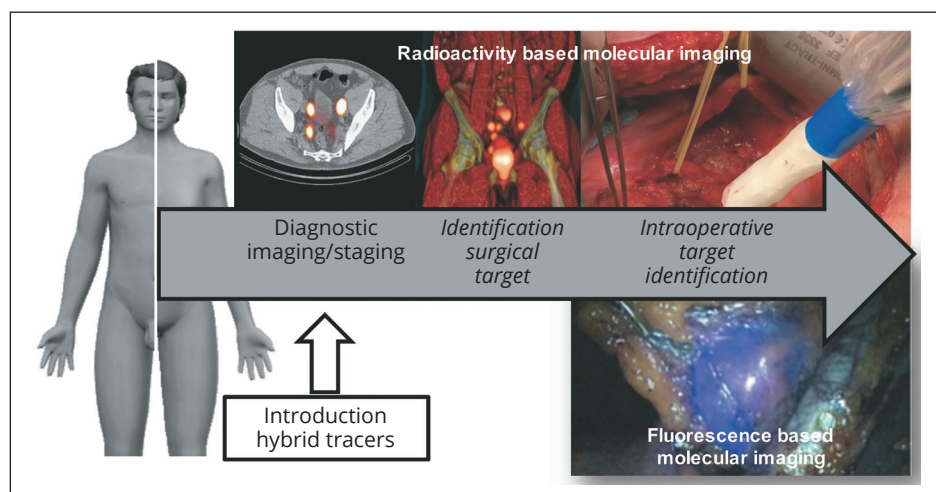


TABLE I.—*Fluorescent tracers applied in the clinical setting. Modified from van Beurden et al.<sup>11</sup>*

Tracer name	Tracer type	Application	Ex/em Wavelength (nm)	Number of patients	Clinical routine Y/N
ICG	Unconjugated fluorescent dye	Lymphangiography, <sup>12</sup> sentinel node imaging <sup>13</sup>	807/822 (FBS, HEPES)	N.≥1500	Approved routine fluorescence use: angiography
Fluorescein	Unconjugated fluorescent dye	Ureter visualization, <sup>14</sup> lymphangiography <sup>15</sup>	488/515 (PBS)	N.≥1000	Approved routine fluorescence use: angiography
Methylene blue	Unconjugated fluorescent dye	Ureter visualization <sup>16</sup>	665/688 (FBS/HEPES)	N.=24	No; multiple studies
EC17 (Folate-FITC)	Folate-targeting small molecule	Ovarian carcinoma <sup>17</sup>	488/515 (PBS)	N.=66	No; single study
OTL38 (Folate-800CW)	Folate-targeting small molecule	Ovarian carcinoma, <sup>18</sup> endometrial cancer <sup>19</sup>	774/788	N.=455	No; multiple studies
EMI-137 (GE137)	C-Met targeting peptide	Penile cancer <sup>20</sup>	650/670	N.=17	No; single study
IR800 IAB2M	PSMA-targeting minibody	Prostate cancer <sup>21</sup>	774/788	N.=120	No; single study
CW800-Bevacizumab	VEGF-targeting Antibody	Endometriosis <sup>21</sup>	774/788	N.=20 ( <i>ex vivo</i> ) N.=55	No; single study

receptor-targeted tracers (Table I).<sup>11-21</sup> In this context, different targeting vectors are currently applied, ranging from small molecules to peptides, minibodies and antibodies, with applications in ovarian and endometrial cancer (folate targeting),<sup>17-19</sup> penile cancer (c-Met targeting),<sup>20</sup> prostate cancer (PSMA-targeting)<sup>21</sup> and endometriosis (VEGF targeting).<sup>21</sup> In clinical studies, the focus is still mainly placed on the use of near-infrared (NIR) dyes ( $\lambda_{em}$  700-950 nm, *e.g.*, ICG or 800CW), although dyes of lower wavelengths (*e.g.*, far-red dyes such as Cy5 [ $\lambda_{em}$  650-670 nm]) are also being increasingly used.<sup>21, 22</sup>

At first glance, it seems a straightforward approach to combine nuclear and fluorescence imaging *via* the use of two different tracers. However, differences in their respective *in-vivo* biodistributions may increase the risk of discrepancies between the individual findings.<sup>23</sup> This can be prevented by designing a tracer that contains both a radio- and fluorescence label, resulting in a novel tracer with hybrid features. Obviously, the combinations between isotopes and fluorescent dyes are seemingly endless, but addition of a fluorescent dye to an already clinically established radiotracer has the highest potential of allowing a relatively fast clinical translation.

### Fluorescence guidance in urogenital malignancies

Clinically, SN imaging has served as a perfect starting point for the clinical introduction of novel image-guidance concepts such as the use of fluorescent and even hybrid tracers. Based on this convincing proof-of-concept that demonstrates the superiority of surgical accuracy when combining fluorescence- and radioguidance, current ef-

forts are focused on implementing receptor-targeted hybrid imaging and surgical guidance. Both these concepts will be discussed in more detail below.

### SN imaging

Administration of fluid in general (or, more specifically in this context, a radiotracer preparation), within the interstitial space of tissue predominantly results in drainage of the injected compound *via* the lymphatic system. This concept has been exploited to identify lymph node basins that are related to a specific anatomical location, so-called lymphatic mapping. The ability to accurately identify lymph nodes that accumulate radioactivity after injection of a radioactive tracer has driven the development of selective biopsy/excision of the first lymph node(s) draining directly from a tumor, the so-called SNs. Assuming that metastatic spread follows a sequential pattern through lymph nodes in the lymphatic system, histopathological examination of the excised SNs would allow identification of early lymph node invasion (micrometastases). As such, the SN biopsy procedure provides a particularly valuable tool to identify early metastatic spread in clinically node negative patients, while sparing them from a potentially unnecessary radical lymph node dissection with all its (co)morbidities if the SN does not contain tumor cells.

For clinically node-negative patients with an increased risk of nodal metastases (stage  $\geq$ T1G2 for penile cancer and  $<4$  cm for squamous cell carcinoma of the vulva), SN procedures are recommended. Here, management of inguinal lymph nodes is crucial for prognosis and helps re-



TABLE II.—Hybrid tracers applied in the clinical setting. Modified from van Leeuwen et al.<sup>7</sup>

Tracer name	Tracer type	Application	Wavelength	Number of patients	Clinical routine Y/N
ICG- <sup>99m</sup> Tc-nanocolloid <sup>6, 30, 31</sup>	Albumin colloid	Sentinel node imaging, radioguided occult lesion localization, tumour margin delineation	802/870	>1500	Y
<sup>125</sup> I-methylene blue <sup>32</sup>	Fluorescent dye	Sentinel lymph node	665/668	12	N
<sup>111</sup> In-DOTA-girentuximab-RDye800CW <sup>33</sup>	Antibody	Renal cancer	775/792	15	N
<sup>68</sup> Ga-Glu-urea-Lys-(HE) <sub>3</sub> -HBED-CC-RDye800CW <sup>34</sup>	Peptide	Prostate cancer	775/792	1	N

duce the complication rates by minimizing the amount of dissected inguinal lymph nodes.<sup>24, 25</sup> SN detection in other malignancies, such as prostate, cervical, endometrial and bladder cancer, is currently only performed in a research setting or as local standard treatment.<sup>4, 26, 27</sup>

Initially, fluorescent dyes such as ICG and Methylene blue (also defined as “blue dye”) have been added as separate components during local tracer injection to provide additional visual assistance during radioguided SN resection.<sup>28, 29</sup> Differences in the drainage kinetics between the relatively small dye molecules and the traditional 50-70nm radiocolloids require separate injections at different timepoints prior to and during the intervention. This can be circumvented by using hybrid analogs such as ICG-<sup>99m</sup>Tc-nanocolloid (Table II)<sup>6, 7, 30-34</sup> or <sup>125</sup>I -methylene blue,<sup>32</sup> combining both “signaling units” in one and the same molecule with a defined clearance pattern. Of all the hybrid tracers in human applications, ICG-<sup>99m</sup>Tc-nanocolloid is the most frequently and widely applied (>1500 patients, multiple cancer types).<sup>6, 30, 31, 35-38</sup> Recently, several large patient cohort studies were described wherein this tracer was used to assess the added value of fluorescence guidance in radioguided surgery.<sup>6, 36, 37</sup>

When implementing a novel hybrid tracer, verification of its use compared to the current clinical standard, and in this case with the parental radiotracer, is of course in-

strumental. Comparison between the parental radiotracer <sup>99m</sup>Tc-nanocolloid and ICG-<sup>99m</sup>Tc-nanocolloid has shown no differences in drainage patterns and SN identification rate between these tracers during preoperative SPECT imaging.<sup>37-39</sup>

However, when focusing on intraoperative optical guidance, recent reports reveal that the use of ICG-<sup>99m</sup>Tc-nanocolloid improves the intraoperative SN identification rate compared to other visual detection methods such as blue dye<sup>6, 36</sup> and unconjugated ICG.<sup>38</sup> In a study in 400 penile cancer patients Dell’Oglio *et al.*<sup>36</sup> showed that fluorescence imaging using ICG-<sup>99m</sup>Tc-nanocolloid yielded a 39% higher SN identification rate compared to blue dye (Figure 2).<sup>36</sup> Moreover, of the tumor positive nodes, 100% were intraoperatively visualized by fluorescence imaging, while only 84% of the positive nodes were stained blue. Similar findings were recorded for penile cancer by Klein Jan *et al.* (54% higher number of intraoperatively identified SNs with fluorescence compared to blue dye)<sup>6</sup> but also for vulvar cancer (38%;<sup>6</sup>) and cervical cancer (46.4%).<sup>30</sup> Also important, the use of this tracer did not result in staining of the surgical field during LN excision, while at the same time eliminating the requirement of an additional tracer injection (as required during the use of two separate tracers).<sup>36</sup> Comparison between ICG-<sup>99m</sup>Tc-nanocolloid and unconjugated ICG in prostate cancer patients also revealed superi-

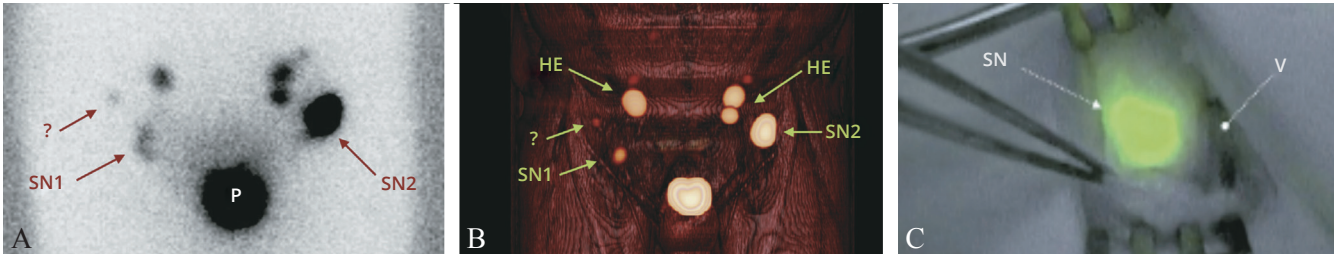


Figure 2.—Sentinel node imaging using the hybrid tracer ICG-<sup>99m</sup>Tc-nanocolloid. Preoperative A) lymphoscintigraphy; and B) SPECT/CT used for sentinel node identification and surgical planning. C) Intraoperative fluorescence imaging showing the sentinel node. Modified from Dell’Oglio *et al.*<sup>36</sup> SN: sentinel node; P: injection site in prostate; HE: higher echelon node; V: vein.

This document is protected by international copyright laws. No additional reproduction is authorized. It is permitted for personal use to download and save only one file and print only one copy of this Article. It is not permitted to make additional copies (either sporadically or systematically, either printed or electronic) of the Article for any purpose. It is not permitted to distribute the electronic copy of the article through online internet and/or intranet file sharing systems, electronic mailing or any other means which may allow access to the Article. The use of all or any part of the Article for any Commercial Use is not permitted. The production of derivative works from the Article is not permitted. It is not permitted to remove, cover, overlay, obscure, block, or change any copyright notices or terms of use which the Publisher may post on the Article. It is not permitted to frame or use framing techniques to enclose any trademark, logo, or other proprietary information of the Publisher.

ority of the hybrid agent, with the hybrid tracer providing substantially higher SN identification rates under fluorescence guidance (75.9% vs. 51.8%) and higher precision in the sparing of non-SNs during surgery.<sup>38</sup> Of note, the use of unconjugated ICG resulted in the removal of a 24% higher number of non-SNs compared to ICG-<sup>99m</sup>Tc-nanocolloid.

In accordance with these findings, the study by Meershoek *et al.* also provides indisputable evidence that fluorescence guidance alone without prior knowledge of the approximate location of the target lesion can result in incomplete LN resection, underlining the importance of a preoperative roadmap as provided by nuclear imaging.<sup>38</sup> In this study, operating surgeons were blinded for the preoperative SPECT/CT results obtained with ICG-<sup>99m</sup>Tc-nanocolloid until completion of fluorescence-guided SN identification and removal, whereafter the preoperative images were used to validate that all SNs were indeed removed. Combined radio- and fluorescence guidance was used to remove the missed SNs. This approach revealed that fluorescence-guided pelvic nodal surgery underestimated the number of SNs in 60-80% of patients. Despite the missed SNs under fluorescence guidance alone, the location of SNs identified using ICG-<sup>99m</sup>Tc-nanocolloid could be directly correlated to the location of the SNs as identified on preoperative SPECT/CT.<sup>40</sup> Moreover, the preoperative imaging roadmap provided by SPECT/CT was shown to enhance the intraoperative detection of prostate related SNs in more ectopic locations in 68% of patients. The synergistic value of combined radio-and fluorescence guidance becomes even more evident when SNs are located in close proximity to the injection site: in such cases, radioguidance does not allow distinction between the two, while fluorescence guidance does enable precise resection.<sup>6</sup> The other way round, when SNs are located deeper than 0.5-1 cm beneath the tissue surface, fluorescence guidance becomes unreliable while the radioactive signature then becomes instrumental in intraoperative SN identification.<sup>6</sup>

Obviously, these well documented improvements in intraoperative SN identification are already a huge step forward, but long-term follow-up is critical for assessment of the therapeutic effect of the hybrid SN biopsy concept. As the technique is still relatively new, long-term follow-up in large patient cohorts is currently still ongoing. However, the first results obtained from such studies do show promising results. In a retrospective analysis of prospectively collected data in 1680 prostate cancer patients (including a 3-year follow-up) Mazzone *et al.* revealed that the use of ICG-<sup>99m</sup>Tc-nanocolloid not only improved the detection of cancer-positive SNs, but the SN biopsy technique po-

tentially also has a positive effect on (biochemical) recurrence rates compared to an extended lymph node dissection (ePLND).<sup>37</sup>

### Tumor targeted imaging

In contrast to lymphatic mapping approaches that follow physiological drainage properties regardless the presence of metastases, a tumor-targeted approach would enable direct visualization of tumor cells. Here, intraoperative visualization of the primary tumor and ultimately, (lymphatic) metastases after intravenous tracer administration would be highly beneficial in current clinical practice.<sup>4, 41</sup> Although a variety of target-specific (primarily receptor- or enzyme-targeted) radiotracers has become available,<sup>42, 43</sup> their clinical implementation is still mainly limited to preoperative imaging. A prime example of tumor-targeted preoperative lesion identification in urology focusses on targeting of the prostate specific membrane antigen (PSMA). PET imaging using <sup>68</sup>Ga-PSMA tracers based on the EuK inhibitor has demonstrated that relatively small lymphatic metastases down to 2-4 mm in diameter could be detected in prostate cancer patients.<sup>44-48</sup> In this setting, a detection efficacy for lymph node metastases at a short axis diameter of 2.3 mm was shown to be 50%, increasing to 90% for metastases with a diameter of 4.5 mm.<sup>48</sup>

The success of <sup>68</sup>Ga-labeled PSMA ligands in nuclear imaging has also triggered the interest for a corresponding application in image-guided surgery. To this end, <sup>111</sup>In-PSMA and <sup>99m</sup>Tc-PSMA tracers have been developed that enable intraoperative radioguidance in salvage PLND in prostate cancer patients based on conventional gamma tracing.<sup>49, 50</sup> Preoperative <sup>68</sup>Ga-PSMA-based PET/CT imaging (which has a superior resolution and sensitivity compared to PSMA-SPECT) provides a roadmap that allows patient selection based on the presence of oligometastatic disease in lymph nodes.<sup>41</sup> This approach does, however, require additional injection with the <sup>111</sup>In- or <sup>99m</sup>Tc-PSMA tracer prior to the surgical intervention.<sup>41</sup> Given comparable biodistribution patterns and tumor uptake characteristics of the PET agent and the radiotracer used for radioguidance, this dual-tracer strategy has proven to allow reliable radio-guided resection of lymph metastases that were identified on PET/CT.<sup>51</sup>

Interestingly, tumor-targeted fluorescence guidance has mainly been focused on the resection of the primary tumor<sup>17-19</sup> and remains mostly based on first-in-human proof-of-principle application in small patient groups. To date, only a limited number of targets have been evaluated in phase I studies in urological and gynecological appli-



TABLE III.—Multicolor combinations applied in the clinical setting. Modified from van Beurden et al.<sup>11</sup>

Tracer combination	Tracer types	Application	Wavelength (ex/em)	Number of patients	Clinical routine Y/N
Fluorescein PpIX <sup>52</sup>	Unconjugated fluorescent dyes	trans urethral dissection bladder cancer	488/512 404/634	84 (21 <i>ex vivo</i> )	N
ICG- <sup>99m</sup> Tc-nanocolloid, Fluorescein <sup>53</sup>	Albumin colloid, Unconjugated fluorescent dye	Visualization of SN and the associated lymph ducts	807/822 488/512	10	N
PpIX, Autofluorescence <sup>54</sup>	Unconjugated fluorescent dye	malignant bladder lesions	404/634	10	N
Methylene blue, ICG <sup>55</sup>	Unconjugated fluorescent dyes	association between injection site and SN detection	665/668 807/822	2	N
ICG- <sup>99m</sup> Tc-nanocolloid, EMI-137 <sup>20</sup>	Albumin colloid, Peptide	Combined imaging SN and primary penile cancer	807/822 650/670	15 (10 <i>ex vivo</i> )	N

cations: Folate in ovarian and endometrial cancer (Table I),<sup>11-21</sup> C-Met in penile cancer (Table I),<sup>11-21</sup> VEGF in endometriosis (Table I),<sup>11-21</sup> carbonic anhydrase IX (CAIX) in renal cancer and PSMA in prostate cancer (Table I).<sup>11-21</sup> In a clinical feasibility study in twelve patients, Hoogstins *et al.* showed that the folate receptor-targeting fluorescent tracer OTL-38 enabled intraoperative visualization of tumor and metastatic lesions. Moreover, fluorescence imaging allowed visualization of a 29% higher number of lesions that were not identified using standard evaluation and/or palpation.<sup>18</sup> A different folate-targeting fluorescent tracer derivative, Folate-FITC, showed that intraoperative fluorescence imaging enabled staging and debulking surgery in ovarian cancer patients (5 patients).<sup>17</sup>

De Vries *et al.* used *ex-vivo* assessment of fresh surgical penile cancer samples (through incubation in a solution containing the c-Met targeted fluorescent ligand EMI-137) in order to predict *in-vivo* feasibility of c-Met targeting in penile cancer patients (Table III).<sup>11, 20, 52-55</sup> *Ex-vivo* and *in-vivo* c-Met targeting was shown to be successful in all 15 patients (10 *ex vivo*, 5 *in vivo*) (Figure 3).<sup>20</sup> *In vivo*, the c-Met targeted visualization of the primary tumor was combined with SN imaging using ICG-<sup>99m</sup>Tc-nanocolloid (in 3 patients), showing the c-Met targeted approach (Cy5-based; Figure 3B-D)<sup>20</sup> was compatible with lymphatic mapping (ICG-based; Figure 3E)<sup>20</sup> performed in the same patient using multicolor fluorescence imaging. In these patients, preoperatively identified SNs (Figure 3E insert)<sup>20</sup> were removed using a combination of radio- and fluorescence guidance. Fluorescence imaging prior to resection of the SN enabled visualization of both lymphatic drainage from the injection site (Figure 3E)<sup>20</sup> and superficially located SNs (Figure 3E, encircled in white).<sup>20</sup> No tumor-positive SNs were identified, therefore presence of tumor cells based on c-Met targeting could not be assessed using targeted fluorescence imaging. However, these results, together with a

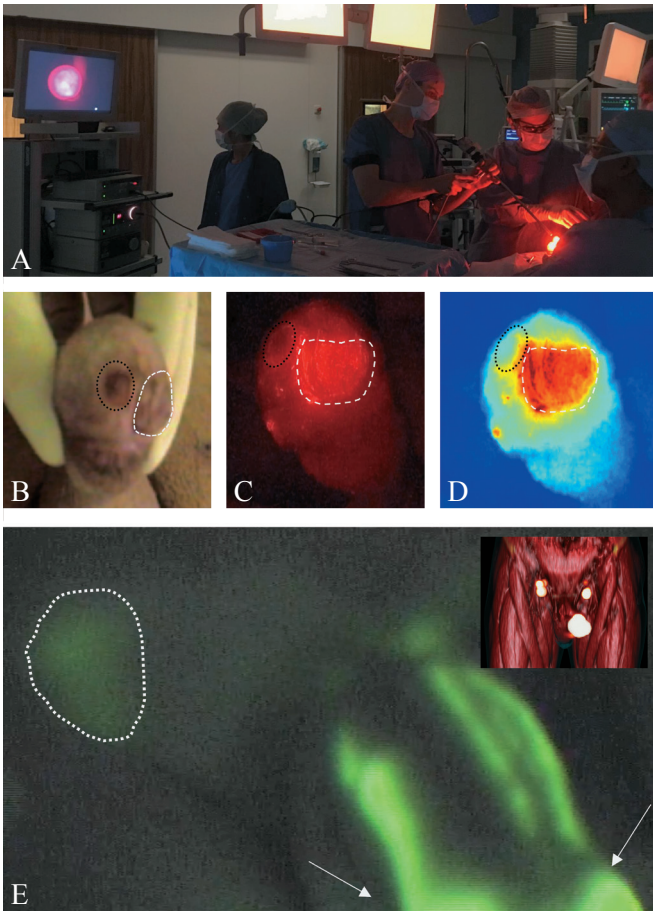


Figure 3.—Combined tumor targeted and multi-color imaging. A) Overview of the surgical theatre during intraoperative laparoscopic fluorescence imaging. B) Tumor targeted imaging in penile cancer after intravenous administration of the fluorescent c-Met targeting tracer EMI-37 using: white light; and C) fluorescence imaging. D) Real-time image processing was shown to enable margin identification (tumor encircled in white). E) Sentinel node imaging in the same patient after local administration of ICG-<sup>99m</sup>Tc-nanocolloid (injection site: white arrow, sentinel node encircled in white). Insert shows the corresponding preoperative SPECT/CT. Modified from de Vries *et al.*<sup>20</sup>

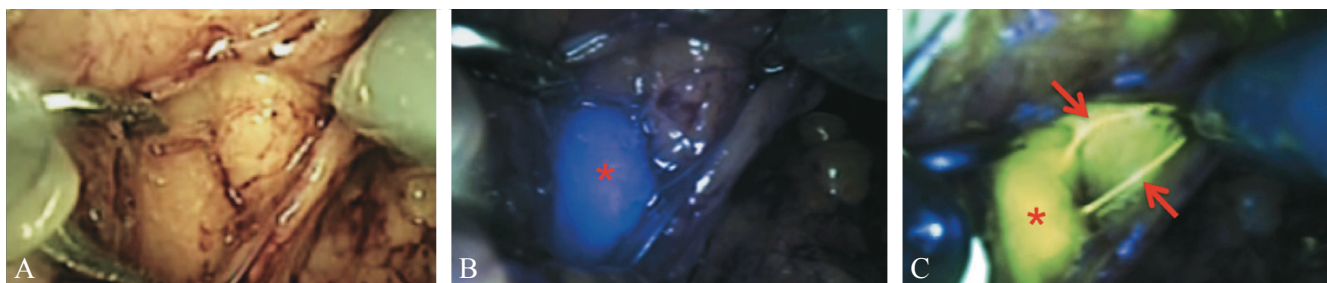


Figure 4.—Multi-wavelength imaging of the lymphatic system. A) White light imaging of the surgical field of view. B) Fluorescence imaging enabling visualization of a sentinel node (asterisk, in red) based on ICG-99mTc-nanocolloid; and C) identification of the same node and draining lymph vessels (arrow, in red). Modified from van den Berg *et al.*<sup>53</sup>

single case-report describing the use of a hybrid PSMA-targeting tracer ( $^{68}\text{Ga}$ -Glu-urea-Lys-[HE]<sub>3</sub>-HBED-CC-IRDye800CW) (Table II)<sup>6, 7, 30-34</sup> and a feasibility study in fifteen renal cancer patients using the hybrid CAIX targeting tracer ( $^{111}\text{In}$ -DOTA-girentuximab-IRDye800CW) (Table II)<sup>6, 7, 30-34</sup> demonstrate the potential of combined preoperative nuclear imaging and intraoperative fluorescence/radioguidance, as currently applied for lymphatic applications. The latter is clearly gaining momentum, as a great number of hybrid tumor-targeted tracers are currently being developed for a variety of different targets.<sup>56-59</sup> Obviously, studies in large(r) patient groups will be required to assess the additional value of such tumor-targeted approaches.

## Future perspectives

### Multicolor imaging

The study by de Vries *et al.* mentioned above<sup>20</sup> illustrates that while currently fluorescence-guided surgery is mainly focused on visualization of one individual feature, combined use of complementary fluorescent tracers with different excitation and emission spectra (colors) could help provide valuable additional information: it may allow intraoperative differentiation between the most important surgical targets and surrounding vital structures (e.g., tumor tissue vs. vasculature, lymph nodes/drainage or nerves) and to detect multiple molecular targets within a single lesion. In literature, a few examples are described that underline the feasibility of this approach in both the preclinical and clinical setting (Table III).<sup>11, 20, 52-55</sup>

In lymphatic imaging, multicolor fluorescence imaging was shown to help simplify the heterogeneity of the complex anatomies in the pelvic region by highlighting the SNs that could possibly harbor metastases with one fluorescent color, while also visualizing non tumor draining lymphatic ducts with a different fluorescent color, so that unnecessary damaging these structures can be avoided.

The feasibility of this approach was successfully shown in a porcine model;<sup>60</sup> herein the use of a combination of Fluorescein and ICG-nanocolloid enabled discrimination between these different networks within the lymphatic system (Figure 4).<sup>53</sup> Administration of Fluorescein in the hind leg was used to visualize the intra-abdominal lymph drainage of the lower limbs, while ICG-nanocolloid allowed identification of prostate-related SNs after intra-prostatic tracer administration. Simultaneous multi-wavelength fluorescence imaging of both dyes during robotic surgery was performed with a standard Firefly laparoscope (da Vinci Si and Xi, Intuitive Surgical) allowing discrimination between the lymphatic drainage of the limbs and prostate without any overlap in signal<sup>60</sup>. A similar approach in was assessed in prostate cancer patients (Table III),<sup>11, 20, 52-55</sup> wherein the different kinetics of ICG-<sup>99m</sup>Tc-nanocolloid (preoperative and intraoperative SN identification) and fluorescein (intraoperative visualization of lymphatic vessels) were successfully exploited to provide additional intraoperative guidance.

These initial steps encourage further development and expansion of the multi-wavelength approach to other indications.<sup>11</sup> And while clinical examples are still limited,<sup>20, 53</sup> preclinical developments already allow discrimination between healthy parenchyma and colorectal liver metastasis based on fluorescein and ICG<sup>61</sup> and tumor detection (SGM-101) as well as the identification of intrahepatic bile ducts and/or vasculature (ICG) in the reconstructive part of hepatic surgery<sup>62</sup> in murine models. The use of “activatable” dyes<sup>63</sup> and nerve specific tracers<sup>64-69</sup> could provide additional possibilities for discrimination between healthy and diseased tissue using multi-wavelength fluorescence imaging.<sup>11</sup>

## Conclusions

The complementary nature of combined radio- and fluorescence guidance provided by hybrid tracers has shown



to be beneficial for improved intraoperative identification of tumor lesions and sentinel lymph nodes and has a potential beneficial effect on (biochemical) recurrence rates in SN biopsy applications in urogenital malignancies. Increasing availability of fluorescent and hybrid receptor-targeted tracers and currently emerging multi-wavelength approaches further underline the bright and colorful future that lies ahead when fully exploiting the inherent possibilities for intraoperative discrimination between diseased and healthy tissue.

## References

- Lakhman Y, Nougaret S, Miccò M, Scelzo C, Vargas HA, Sosa RE, *et al.* Role of MR Imaging and FDG PET/CT in Selection and Follow-up of Patients Treated with Pelvic Exenteration for Gynecologic Malignancies. *Radiographics* 2015;35:1295–313.
- Mehralivand S, van der Poel H, Winter A, Choyke PL, Pinto PA, Turkbey B. Sentinel lymph node imaging in urologic oncology. *Transl Androl Urol* 2018;7:887–902.
- Mendhiratta N, Taneja SS, Rosenkrantz AB. The role of MRI in prostate cancer diagnosis and management. *Future Oncol* 2016;12:2431–43.
- van Leeuwen FW, Winter A, van Der Poel HG, Eiber M, Suardi N, Graefen M, *et al.* Technologies for image-guided surgery for managing lymphatic metastases in prostate cancer. *Nat Rev Urol* 2019;16:159–71.
- Bugby SL, Lees JE, Perkins AC. Hybrid intraoperative imaging techniques in radioguided surgery: present clinical applications and future outlook. *Clin Transl Imaging* 2017;5:323–41.
- KleinJan GH, van Werkhoven E, van den Berg NS, Karakullukcu MB, Zijlmans HJ, van der Hage JA, *et al.* The best of both worlds: a hybrid approach for optimal pre- and intraoperative identification of sentinel lymph nodes. *Eur J Nucl Med Mol Imaging* 2018;45:1915–25.
- van Leeuwen FW, Schottelius M, Brouwer OR, Vidal-Sicart S, Achillefu S, Klode J, *et al.* Trending: Radioactive and Fluorescent Bimodal/Hybrid Tracers as Multiplexing Solutions for Surgical Guidance. *J Nucl Med* 2020;61:13–9.
- Tian Y, Halle J, Wojdyr M, Sahoo D, Scheblykin IG. Quantitative measurement of fluorescence brightness of single molecules. *Methods Appl Fluoresc* 2014;2:035003.
- Spa SJ, Hensbergen AW, van der Wal S, Kuil J, van Leeuwen FW. The influence of systematic structure alterations on the photo-physical properties and conjugation characteristics of asymmetric cyanine 5 dyes. *Dyes Pigments* 2018;152:19–28.
- van der Wal S, Kuil J, Valentijn AR, van Leeuwen FW. Synthesis and systematic evaluation of symmetrically sulfonated centrally Ce C bonded cyanine near-infrared dyes for protein labeling. *Dyes Pigments* 2016;132:7–19.
- van Beurden F, van Willigen DM, Vojnovic B, van Oosterom MN, Brouwer OR, der Poel HG, *et al.* Multi-Wavelength Fluorescence in Image-Guided Surgery, Clinical Feasibility and Future Perspectives. *Mol Imaging* 2020;19:1536012120962333.
- Unno N, Inuzuka K, Suzuki M, Yamamoto N, Sagara D, Nishiyama M, *et al.* Preliminary experience with a novel fluorescence lymphography using indocyanine green in patients with secondary lymphedema. *J Vasc Surg* 2007;45:1016–21.
- Kitai T, Inomoto T, Miwa M, Shikayama T. Fluorescence navigation with indocyanine green for detecting sentinel lymph nodes in breast cancer. *Breast Cancer* 2005;12:211–5.
- Verbeek FP, van der Vorst JR, Schaafsma BE, Swijnenburg RJ, Gaarenstroom KN, Elzevier HW, *et al.* Intraoperative near infrared fluorescence guided identification of the ureters using low dose methylene blue: a first in human experience. *J Urol* 2013;190:574–9.
- Cooper SG, Maitem AN, Richman AH. Fluorescein labeling of lymphatic vessels for lymphangiography. *Radiology* 1988;167:559–60.
- Udshmadshuridze NS, Asikuri TO. [Intra-operative imaging of the ureter with sodium fluorescein]. *Z Urol Nephrol* 1988;81:635–9. [German]
- van Dam GM, Themelis G, Crane LM, Harlaar NJ, Pleijhuis RG, Kelder W, *et al.* Intraoperative tumor-specific fluorescence imaging in ovarian cancer by folate receptor- $\alpha$  targeting: first in-human results. *Nat Med* 2011;17:1315–9.
- Hoogstins CE, Tummers QR, Gaarenstroom KN, de Kroon CD, Trimbos JB, Bosse T, *et al.* A Novel Tumor-Specific Agent for Intraoperative Near-Infrared Fluorescence Imaging: A Translational Study in Healthy Volunteers and Patients with Ovarian Cancer. *Clin Cancer Res* 2016;22:2929–38.
- Boogerd LS, Hoogstins CE, Gaarenstroom KN, de Kroon CD, Beltman JJ, Bosse T, *et al.* Folate receptor- $\alpha$  targeted near-infrared fluorescence imaging in high-risk endometrial cancer patients: a tissue microarray and clinical feasibility study. *Oncotarget* 2017;9:791–801.
- de Vries HM, Bekers E, van Oosterom MN, Karakullukcu MB, van der Poel HG, van Leeuwen FWB, *et al.* C-MET receptor-targeted fluorescence-guided surgery – first experience in penile squamous cell carcinoma patients, a phase IIa study. *JNM* 2021. [Epub ahead of print]
- Hernot S, van Manen L, Debie P, Mieog JS, Vahrmeijer AL. Latest developments in molecular tracers for fluorescence image-guided cancer surgery. *Lancet Oncol* 2019;20:e354–67.
- Burggraaf J, Kamerling IM, Gordon PB, Schrier L, de Kam ML, Kales AJ, *et al.* Detection of colorectal polyps in humans using an intravenously administered fluorescent peptide targeted against c-Met. *Nat Med* 2015;21:955–61.
- van Leeuwen FW, van der Poel HG. Surgical Guidance in Prostate Cancer: “From Molecule to Man” Translations. *Clin Cancer Res* 2016;22:1304–6.
- Hakenberg OW, Compérat EM, Minhas S, Necchi A, Protzel C, Watkin N. EAU guidelines on penile cancer: 2014 update. *Eur Urol* 2015;67:142–50.
- Kamel MH, Khalil MI, Davis R, Spiess PE. Management of the Clinically Negative (cN0) Groin Penile Cancer Patient: A Review. *Urology* 2019;131:5–13.
- Giammarile F, Schilling C, Gnanasegaran G, Bal C, Oyen WJ, Rubello D, *et al.* The EANM practical guidelines for sentinel lymph node localisation in oral cavity squamous cell carcinoma. *Eur J Nucl Med Mol Imaging* 2019;46:623–37.
- Skanjeti A, Dhompas A, Paschetta C, Tordo J, Giammarile F. Sentinel Node Mapping in Gynecologic Cancers: A Comprehensive Review. *Semin Nucl Med* 2019;49:521–33.
- Aoun F, Albisinni S, Zanaty M, Hassan T, Janetschek G, van Velthoven R. Indocyanine green fluorescence-guided sentinel lymph node identification in urologic cancers: a systematic review and meta-analysis. *Minerva Urol Nefrol* 2018;70:361–9.
- Rocha A, Dominguez AM, Lécure F, Bourdel N. Indocyanine green and infrared fluorescence in detection of sentinel lymph nodes in endometrial and cervical cancer staging - a systematic review. *Eur J Obstet Gynecol Reprod Biol* 2016;206:213–9.
- Paredes P, Vidal-Sicart S, Campos F, Tapias A, Sánchez N, Martínez S, *et al.* Role of ICG-99mTc-nanocolloid for sentinel lymph node detection in cervical cancer: a pilot study. *Eur J Nucl Med Mol Imaging* 2017;44:1853–61.
- Stoffels I, Leyh J, Pöppel T, Schadendorf D, Klode J. Evaluation of a radioactive and fluorescent hybrid tracer for sentinel lymph node biopsy in head and neck malignancies: prospective randomized clinical trial to compare ICG-(99m)Tc-nanocolloid hybrid tracer versus (99m)Tc-nanocolloid. *Eur J Nucl Med Mol Imaging* 2015;42:1631–8.

32. Cundiff JD, Wang YZ, Espenan G, Maloney T, Camp A, Lazarus L, *et al.* A phase I/II trial of 125I methylene blue for one-stage sentinel lymph node biopsy. *Ann Surg* 2007;245:290–6.
33. Hekman MC, Rijpkema M, Muselaers CH, Oosterwijk E, Hulsbergen-Van de Kaa CA, Boerman OC, *et al.* Tumor-targeted Dual-modality Imaging to Improve Intraoperative Visualization of Clear Cell Renal Cell Carcinoma: A First in Man Study. *Theranostics* 2018;8:2161–70.
34. Eder AC, Omrane MA, Stadlbauer S, Roscher M, Khoder WY, Gratzke C, *et al.* The PSMA-11-derived hybrid molecule PSMA-914 specifically identifies prostate cancer by preoperative PET/CT and intraoperative fluorescence imaging. *Eur J Nucl Med Mol Imaging* 2021;48:2057–8.
35. Christensen A, Juhl K, Charabi B, Mortensen J, Kiss K, Kjær A, *et al.* Feasibility of Real-Time Near-Infrared Fluorescence Tracer Imaging in Sentinel Node Biopsy for Oral Cavity Cancer Patients. *Ann Surg Oncol* 2016;23:565–72.
36. Dell'Oglio P, de Vries HM, Mazzone E, KleinJan GH, Donswijk ML, van der Poel HG, *et al.* Hybrid Indocyanine Green-99mTc-nanocolloid for Single-photon Emission Computed Tomography and Combined Radio- and Fluorescence-guided Sentinel Node Biopsy in Penile Cancer: Results of 740 Inguinal Basins Assessed at a Single Institution. *Eur Urol* 2020;78:865–72.
37. Mazzone E, Dell'Oglio P, Grivas N, Wit E, Donswijk M, Briganti A, *et al.* Diagnostic Value, Oncological Outcomes And Safety Profile Of Image-Guided Surgery Technologies During Robot-Assisted Lymph Node Dissection with Sentinel Node Biopsy For Prostate Cancer. *J Nucl Med* 2021;jnumed.120.259788. [Epub ahead of print]
38. Meershoek P, Buckle T, van Oosterom MN, KleinJan GH, van der Poel HG, van Leeuwen FW. Can Intraoperative Fluorescence Imaging Identify All Lesions While the Road Map Created by Preoperative Nuclear Imaging Is Masked? *J Nucl Med* 2020;61:834–41.
39. Brouwer OR, Buckle T, Vermeeren L, Klop WM, Balm AJ, van der Poel HG, *et al.* Comparing the hybrid fluorescent-radioactive tracer indocyanine green-99mTc-nanocolloid with 99mTc-nanocolloid for sentinel node identification: a validation study using lymphoscintigraphy and SPECT/CT. *J Nucl Med* 2012;53:1034–40.
40. Soergel P, Kirschke J, Klapdor R, Derlin T, Hillemanns P, Hertel H. Sentinel lymphadenectomy in cervical cancer using near infrared fluorescence from indocyanine green combined with technetium-99m-nanocolloid. *Lasers Surg Med* 2018;50:994–1001.
41. Maurer T, Weirich G, Schottelius M, Weineisen M, Frisch B, Okur A, *et al.* Prostate-specific membrane antigen-radioguided surgery for metastatic lymph nodes in prostate cancer. *Eur Urol* 2015;68:530–4.
42. Mankoff DA, Link JM, Linden HM, Sundararajan L, Krohn KA. Tumor receptor imaging. *J Nucl Med* 2008;49(Suppl 2):149S–63S.
43. Van Den Bossche B, Van de Wiele C. Receptor imaging in oncology by means of nuclear medicine: current status. *J Clin Oncol* 2004;22:3593–607.
44. Li R, Ravizzini GC, Gorin MA, Maurer T, Eiber M, Cooperberg MR, *et al.* The use of PET/CT in prostate cancer. *Prostate Cancer Prostatic Dis* 2018;21:4–21.
45. Maurer T, Eiber M, Schwaiger M, Gschwend JE. Current use of PSMA-PET in prostate cancer management. *Nat Rev Urol* 2016;13:226–35.
46. Perera M, Papa N, Christidis D, Wetherell D, Hofman MS, Murphy DG, *et al.* Sensitivity, Specificity, and Predictors of Positive 68Ga-Prostate-specific Membrane Antigen Positron Emission Tomography in Advanced Prostate Cancer: A Systematic Review and Meta-analysis. *Eur Urol* 2016;70:926–37.
47. Rauscher I, Düwel C, Haller B, Rischpler C, Heck MM, Gschwend JE, *et al.* Efficacy, Predictive Factors, and Prediction Nomograms for 68Ga-labeled Prostate-specific Membrane Antigen-ligand Positron-emission Tomography/Computed Tomography in Early Biochemical Recurrent Prostate Cancer After Radical Prostatectomy. *Eur Urol* 2018;73:656–61.
48. Jilg CA, Drendel V, Rischke HC, Beck T, Vach W, Schaal K, *et al.* Diagnostic Accuracy of Ga-68-HBED-CC-PSMA-Ligand-PET/CT before Salvage Lymph Node Dissection for Recurrent Prostate Cancer. *Theranostics* 2017;7:1770–80.
49. Robu S, Schottelius M, Eiber M, Maurer T, Gschwend J, Schwaiger M, *et al.* Preclinical Evaluation and First Patient Application of 99mTc-PSMA-I&S for SPECT Imaging and Radioguided Surgery in Prostate Cancer. *J Nucl Med* 2017;58:235–42.
50. Schottelius M, Wirtz M, Eiber M, Maurer T, Wester HJ, [(111)In] PSMA-I&T: expanding the spectrum of PSMA-I&T applications towards SPECT and radioguided surgery. *EJNMMI Res* 2015;5:68.
51. Rauscher I, Düwel C, Wirtz M, Schottelius M, Wester HJ, Schwamborn K, *et al.* Value of 111 In-prostate-specific membrane antigen (PSMA)-radioguided surgery for salvage lymphadenectomy in recurrent prostate cancer: correlation with histopathology and clinical follow-up. *BJU Int* 2017;120:40–7.
52. Marien A, Rock A, Maadarani KE, Francois C, Gosset P, Mauroy B, *et al.* Urothelial Tumors and Dual-Band Imaging: A New Concept in Confocal Laser Endomicroscopy. *J Endourol* 2017;31:538–44.
53. van den Berg NS, Buckle T, KleinJan GH, van der Poel HG, van Leeuwen FW. Multispectral Fluorescence Imaging During Robot-assisted Laparoscopic Sentinel Node Biopsy: A First Step Towards a Fluorescence-based Anatomic Roadmap. *Eur Urol* 2017;72:110–7.
54. Kriegmair MC, Rother J, Grychtol B, Theuring M, Ritter M, Günes C, *et al.* Multiparametric Cystoscopy for Detection of Bladder Cancer Using Real-time Multispectral Imaging. *Eur Urol* 2020;77:251–9.
55. Laios A, Volpi D, Tullis ID, Woodward M, Kennedy S, Pathiraja PN, *et al.* A prospective pilot study of detection of sentinel lymph nodes in gynaecological cancers using a novel near infrared fluorescence imaging system. *BMC Res Notes* 2015;8:608.
56. Hensbergen AW, van Willigen DM, van Beurden F, van Leeuwen PJ, Buckle T, Schottelius M, *et al.* Image-Guided Surgery: Are We Getting the Most Out of Small-Molecule Prostate-Specific-Membrane-Antigen-Targeted Tracers? *Bioconjug Chem* 2020;31:375–95.
57. Kelderhouse LE, Chelvam V, Wayua C, Mahalingam S, Poh S, Kularatne SA, *et al.* Development of tumor-targeted near infrared probes for fluorescence guided surgery. *Bioconjug Chem* 2013;24:1075–80.
58. Kuil J, Buckle T, van Leeuwen FW. Imaging agents for the chemokine receptor 4 (CXCR4). *Chem Soc Rev* 2012;41:5239–61.
59. Zhao J, Chen J, Ma S, Liu Q, Huang L, Chen X, *et al.* Recent developments in multimodality fluorescence imaging probes. *Acta Pharm Sin B* 2018;8:320–38.
60. Meershoek P, KleinJan GH, van Oosterom MN, Wit EM, van Willigen DM, Bauwens KP, *et al.* Multispectral-Fluorescence Imaging as a Tool to Separate Healthy from Disease-Related Lymphatic Anatomy During Robot-Assisted Laparoscopy. *J Nucl Med* 2018;59:1757–60.
61. Schneider C, Johnson SP, Gurusamy K, Cook RJ, Desjardins AE, Hawkes DJ, *et al.* Identification of liver metastases with probe-based confocal laser endomicroscopy at two excitation wavelengths. *Lasers Surg Med* 2017;49:280–92.
62. Framery B, Gutowski M, Dumas K, Evrard A, Muller N, Dubois V, *et al.* Toxicity and pharmacokinetic profile of SGM-101, a fluorescent anti-CEA chimeric antibody for fluorescence imaging of tumors in patients. *Toxicol Rep* 2019;6:409–15.
63. Mochida A, Ogata F, Nagaya T, Choyke PL, Kobayashi H. Activatable fluorescent probes in fluorescence-guided surgery: practical considerations. *Bioorg Med Chem* 2018;26:925–30.
64. Buckle T, van der Wal S, van Willigen DM, Aalderink G, KleinJan GH, van Leeuwen FW. Fluorescence background quenching as a means to increase Signal to Background ratio - a proof of concept during Nerve Imaging. *Theranostics* 2020;10:9890–8.
65. Gibbs-Strauss SL, Nasr KA, Fish KM, Khullar O, Ashitate Y, Siclovian TM, *et al.* Nerve-highlighting fluorescent contrast agents for image-guided surgery. *Mol Imaging* 2011;10:91–101.

66. Hingorani DV, Whitney MA, Friedman B, Kwon JK, Crisp JL, Xiong Q, *et al.* Nerve-targeted probes for fluorescence-guided intraoperative imaging. *Theranostics* 2018;8:4226–37.
67. Hussain T, Mastrodimos MB, Raju SC, Glasgow HL, Whitney M, Friedman B, *et al.* Fluorescently labeled peptide increases identification of degenerated facial nerve branches during surgery and improves functional outcome. *PLoS One* 2015;10:e0119600.
68. Walsh EM, Cole D, Tipirneni KE, Bland KI, Udayakumar N, Kas-ten BB, *et al.* Fluorescence Imaging of Nerves During Surgery. *Ann Surg* 2019;270:69–76.
69. Buckle T, Hensbergen AW, van Willigen DM, Bosse F, Bauwens K, Pelger RCM, *et al.* Intraoperative visualization of nerves using a myelin protein-zero specific fluorescent tracer. *Eur J M Nucl Med Mol Imaging Res* 2021;270:69–76. [Epub ahead of print]

*Conflicts of interest.*—The authors certify that there is no conflict of interest with any financial organization regarding the material discussed in the manuscript.

*Funding.*—This work was financially supported by a NWO-TTW-VICI (TTW BGT16141) grant.

*Authors' contributions.*—Hielke-Martijn de Vries, Margret Schottelius, Oscar R. Brouwer and Tessa Buckle have given substantial contributions to study conceptualization, manuscript writing, revision and editing. All authors read and approved the final version of the manuscript.

*History.*—Article first published online: May 31, 2021. - Manuscript accepted: May 14, 2021. - Manuscript revised: May 11, 2021. - Manuscript received: March 10, 2021.